PROCEEDINGS OF SCIENCE

Breaking the universal power law: Advanced models of diffusive shock acceleration in Galactic sources

S. Aerdker,[1,2] **L. Merten,**[1,2] **R. Habegger,**[3] **J. Becker Tjus**[1,2,4] **and E. Zweibel**[3]

[1]*Theoretical Physics IV, Faculty for Physics & Astronomy, Ruhr University Bochum, Germany*

[2]*Ruhr Astroparticle and Plasma Physics Center (RAPP Center), Germany*

[4]*Department of Space, Earth and Environment, Chalmers University of Technology, Gothenburg, Sweden*

Diffusive shock acceleration (DSA) is a promising acceleration process in a hierarchy of sources, reaching from stellar termination to Galaxy cluster shocks. Two of the relevant parameters defining the maximal energy reached at the accelerator are the turbulent magnetic field and the shock's lifetime. In this contribution, we show how time-dependent models in complex geometries and diffusion descriptions beyond a simple scaling in energy, taking structured turbulence and non-linear feedback of the CRs into account, lead to deviations from the universal E^{-2} power law at a strong shock.

By modeling shocks in the Galactic halo, we show how time-dependent transport gives rise to harder energy spectra and the collision of shocks can lead to an enhancement at high energies. The influence of energy-dependent escape including adiabatic cooling on the spectrum is discussed. Harder energy spectra can also be obtained when superdiffusion is considered, which might result from structured turbulence close to astrophysical sources.

All modeling is done in a single framework, a modified version of CRPropa 3.2 based on the integration of stochastic differential equations.

The 39th International Cosmic Ray Conference (ICRC2025)
15–24 July, 2025
Geneva, Switzerland

PoS(ICRC2025)002

1. Introduction

The acceleration processes of high energy cosmic rays (CRs) are still not entirely understood. Diffusive shock acceleration (DSA) remains a promising mechanism at the hierarchy of shocks present in our Galaxy and the Universe. Other processes involve e.g. energy gain in turbulent magnetic fields (second-order Fermi acceleration) [11], shock drift acceleration, or shearing flows [14]. In general, DSA at a one-dimensional, planar and stationary shock leads to the well-known energy spectrum with a -2 power-law in the test particle regime. However, observations of SNRs indicate softer spectra than the -2 spectrum [5], the overall CR energy spectrum shows deviations from the simple -2 prediction, and it has been argued that very hard energy spectra are needed to explain the composition at the highest energies (e.g. [10]). We discuss different models of DSA — at a spherical blast wave, colliding shocks, considering time-dependent escape, as well as the case of superdiffusion — all leading to softer or harder spectra than -2. Superdiffusion, a diffusion process in which the mean-squared displacement of the particles evolves non-linear in time, is modeled by Lévy flights that are characterized by a heavy-tail jump length distribution. In the following we present our methods, based on the integration of stochastic differential equations (SDEs) and discuss the individual DSA models.

2. Methods

All models we discuss below are based on the same framework, a modified version of CRPropa 3.2 [4] with an improved solver for SDEs [12]. In the following, we give a brief overview of the description of diffusive and superdiffusive particle transport with SDEs and focus on the new developments compared to the current public version of CRPropa. In a macroscopic description, assuming an isotropic distribution in momentum p, the differential number density $\mathcal{N} = p^2 f$, with f being the particle distribution function, can be described by a Fokker-Planck equation

$$\frac{\partial \mathcal{N}}{\partial t} = \frac{1}{2}\nabla^2(2\hat{\kappa}\mathcal{N}) - \nabla\left[(\nabla\hat{\kappa} + \mathbf{u})\,\mathcal{N}\right] - \frac{\partial}{\partial p}\left[-\frac{p}{3}(\nabla\cdot\mathbf{u})\mathcal{N}\right] + S \quad , \tag{1}$$

where $\hat{\kappa}$ encodes the spatial diffusion in the presence of turbulent magnetic fields, $\mathbf{u}$ the advection with the background plasma and S any sources and sinks. When writing the transport equation of the form of eq. (1), the stochastic/diffusive terms, characterized by the second derivatives, and deterministic/advective terms, characterized by the first derivatives, are nicely separated. Note that momentum diffusion, second-order Fermi acceleration, is neglected here; it would add another diffusive term (second derivative in momentum) to the equation (see, e.g. [12]).

Any Fokker-Planck equation is equivalent to a set of SDEs, so that eq. (1) can be translated to

$$\mathrm{d}\mathbf{x} = (\mathbf{u} + \nabla\cdot\hat{\kappa})\,\mathrm{d}t + \sqrt{2\hat{\kappa}}\mathrm{d}\mathbf{W}_t \quad , \quad \mathrm{d}p = -\frac{p}{3}\nabla\cdot\mathbf{u}\mathrm{d}t \quad , \tag{2}$$

where the Wiener process $\mathrm{d}\mathbf{W}_t$ is introduced as a stochastic driver for the spatial diffusion. Without momentum diffusion, changes in momentum are given by an ordinary differential equations. The solutions of eq. (2) *sample* the differential number density $\mathcal{N}$ and are called *pseudo-particles* in the following. By integrating many instances of eq. (2) the macroscopic quantity $\mathcal{N}$ can be recovered.

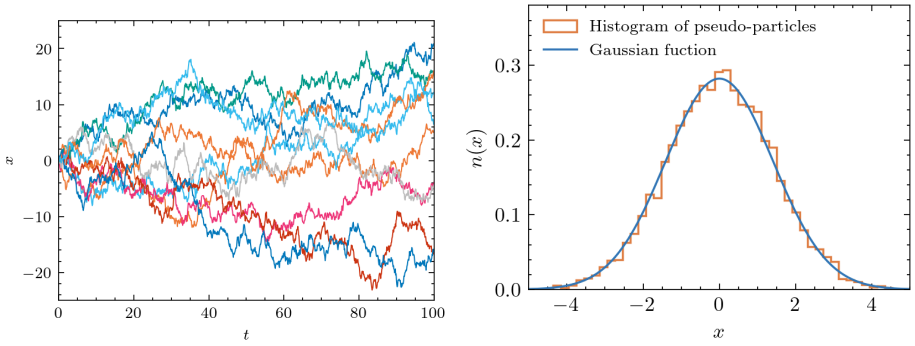

Figure 1: Exemplary pseudo-particle trajectories, solutions of the purely diffusive SDE $\mathrm{d}x = \kappa \mathrm{d}W_t$ (left) and corresponding histogram over space, compared to the Gaussian function solving the related transport equation (right). Fig. courtesy by S. Aerdker, orig. PhD dissertation (2025)

Figure 1 shows pseudo-particle trajectories of the one-dimensional purely diffusive SDE $\mathrm{d}x = \kappa \mathrm{d}W_t$ and the corresponding distribution function, which is a Gaussian function. In this macroscopic picture, DSA results from the interplay of diffusion and adiabatic heating due to the diverging advection **u** at the shock.

2.1 Integrating stochastic differential equations

The SDE eq. (2) is integrated with an Euler-Maruyama scheme, an extension of the well-known Euler scheme where the quantity y is subject to Gaussian noise

$$y_{i,n+1} = y_{i,n} + A_i(y_n, t_n)\Delta t + B_{i,j}(y_n, t_n)\Delta W_{i,n} \quad . \tag{3}$$

Here, the components A_i corresponds to the drift-like terms of the Fokker-Planck equation, B_i represents the diffusive terms where $B_{ij} = \delta_{ij}\sqrt{2\kappa_{ij}}$. The Wiener process is approximated by $\Delta W_n = W(t_{n+1}) - W(t_n)$; Gaussian distributed random numbers with a mean value of zero and variance of the time step Δt. In general, the Euler-Maruyama scheme converges with strong order of $1/2$ and weak order of 1. The weak order is sufficient when the spatial distribution of particles is of interest. However, when modeling shock acceleration the strong order of convergence becomes important, since pseudo-particles have to encounter the region of diverging advection (see [1] details, especially resulting constraints on the time step). When diffusion in momentum is not considered, the change in momentum is deterministic but depends on the stochastic movement of particles leading to a correlated random walk. For the investigation of DSA at blast waves, time-dependent advection fields were added to the modified CRPropa version.[1]

[1] Time-dependent advection fields will become publicly available in the master version of CRPropa soon and are introduced in another contribution, *CRPropa 3.3: Toward a Unified Multi-Messenger Framework from GeV to ZeV Energies.*

2.2 Superdiffusion: Space-fractional transport equation

Superdiffusion can be modeled by space-fractional transport equations

$$\frac{\partial f}{\partial t} = \kappa_\alpha \frac{\partial^\alpha f}{\partial |x|^\alpha} - u(x) \cdot \frac{\partial f}{\partial x} - \frac{p}{3}\frac{\partial u}{\partial x}\frac{\partial f}{\partial p} + S(x,p,t) \quad , \tag{4}$$

where the Riesz-derivative $\partial^\alpha / \partial x^\alpha$ is introduced and the fractional diffusion coefficient κ_α is constant in space.[2] The corresponding stochastic process is given analogously to normal, Gaussian diffusion by a stochastic differential equation

$$\mathrm{d}x = u\mathrm{d}t + \sqrt{2}\kappa_\alpha^{1/\alpha}\mathrm{d}L_{\alpha,t} \quad , \quad \mathrm{d}p = -\frac{p}{3}\frac{\partial u}{\partial x}\mathrm{d}t \quad , \tag{5}$$

where the Wiener process is exchanged by an α-stable Lévy process $\mathrm{d}L_{\alpha,t}$, corresponding to a jump length distribution with heavy power-law tails. The solution of the SDEs is similar to the Euler-Maruyama scheme for normal diffusion, instead of a normal distribution, random numbers are now picked from an α-stable Lévy distribution, for more details we refer to [9]. The fractional dimension describing the heavy power-laws becomes another parameter, characterizing the turbulent motion.

3. Time-dependent acceleration and escape at moving shocks

3.1 Spherical blast waves

We consider the case of a spherical blast wave, moving with the speed $\dot{R}(t)$ into the undisturbed surrounding medium. With the assumption of a surrounding medium with constant density ρ_0, the well-known similarity solution by Sedov, Taylor can be employed, with the shock speed $\dot{R} = \frac{2}{5}\left(\frac{E_{\mathrm{inj}}}{\rho_0}\right)^{1/5} t^{-3/5}$ depending only on the injected energy E_{inj} and density ρ_0. Compared to a stationary shock, the acceleration process is impacted in two ways: the changing rate at which the shock accelerates and the adiabatic cooling in the expanding volume behind the shock. This can impact the spectral slope, as approximated by Drury [8]

$$a = 4\left[1 + (3+b)\left(\frac{\kappa_1}{Ru_1} + \frac{\kappa_2}{Ru_2}\right) + \frac{\kappa_2}{Ru_2}\right] + O(\epsilon^2) \quad , \tag{6}$$

where b describes the injection of particles, assuming $f \propto p^{-a} R(t)^b$. The dimensionless parameter $\epsilon = \kappa/(\dot{R}R)$ is assumed to be small; for $\epsilon \to 0$ the approximation results in the slope at a planar stationary shock, $f \propto p^{-4}$. If, however, the diffusion coefficient is large or the shock radius small compared to the diffusive length scale, the spectral slope can become softer than -4. We use this prediction to verify our time-dependent acceleration models at a Sedov-Taylor blast wave, first considering a constant diffusion coefficient. In order to model shock acceleration with SDEs by integrating eq. (2), the full velocity profile $u(r,t)$ must be smoothed out at the shock, so that pseudo-particles can encounter the shock region (where $\partial u/\partial r < 0$) at a reasonable resolution Δt. In order to still model a discrete shock, the average diffusive step $\sqrt{2\kappa\Delta t}$ must be sufficiently large (see [1] for details). The shock is smoothed out by an hyperbolic tangent and the resulting velocity

[2] The Riesz derivative involves the non-local Riemann-Liouville derivative. See e.g. [2] for the definition.

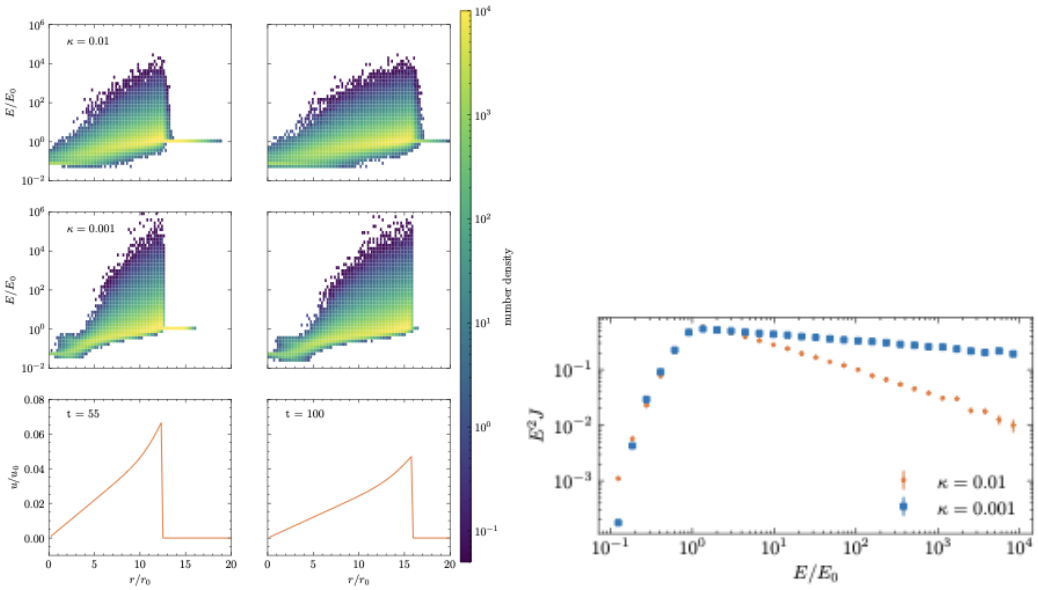

Figure 2: Left: Particle distribution in space and energy for two different diffusion coefficients (top) and shock profile (bottom) at two times: $t = 55, 100$. Right: Energy spectra $J = \mathrm{d}N/\mathrm{d}E$ at the shock, weighted with E^2 at $t = 100$. Figures taken from [3].

profile are shown in fig. 2, together with the resulting particle distributions in space and energy for two different diffusion coefficients. Pseudo-particle are injected mono-energetically with energy E_0 in the upstream region (visible by the horizontal line in the left panel of fig. 2 in front of the shock), the shock moves through the pseudo-particles and accelerates them. The right panel of fig. 2 shows the energy spectrum $J = dN/dE$ at the shock weighted with E^2. We find the softening of the spectrum close to what is predicted in eq. (6), the higher the diffusion coefficient, the softer the spectrum. Considering an energy-dependent diffusion coefficient is more realistic. Particles that are accelerated to higher energies will be have a higher diffusion coefficient which can continuously soften the spectrum towards higher energies. We investigate this at the example of a spherical blast wave that moves into a medium with decreasing density profile. Such a scenario could be found, e.g. when shocks are running out of the Galaxy as a result of Parker-like instabilities (see [7], [3]). The shock profile is then not given by the standard Sedov-Taylor solution with $\dot{R} \propto t^{-3/5}$ but is adjusted by the decreasing density profile, here assumed to be $\rho(r) = \rho_0/r_0 r^{-2}$. In that case the solution becomes critical and $u(r,t)$ for $r < R_{\rm sh}$ is a linear function. For efficient acceleration we assume further that the shock is parallel by adopting a radial magnetic field and considering strong turbulence close to the shock, with the Bohm diffusion coefficient, $\kappa(p,r) = pc^2/(3qB(r))$. The magnetic field strength B decreases with $1/r^2$, so that the mean-free path of the particles increases with r. The magnetic field strength is set to $B_0 = 10\,\mu$G at $r_0 = 1\,$kpc. Note, that the spatial-dependent diffusion coefficient adds the noise-induced drift term $\partial\kappa/\partial r$ to the SDE in eq. (2). Pseudo-particles are injected in the upstream region ($r_0 < r < 60\,$kpc) with an with an energy spectrum E^{-1} from TeV to 100 TeV in the volume $r < 60\,$kpc. The injected energy spectrum is re-weighted in the later analysis to E^{-2}. With $E_{\rm inj} = 10\,E_{\rm SN}$, $r_0 = 1\,$kpc and $\rho_0 = 1\,\mathrm{m_p/m^3}$ the expanding shock reaches a radius of 60 kpc at $t \approx 80\,$Myr. All `Candidates` are protons;

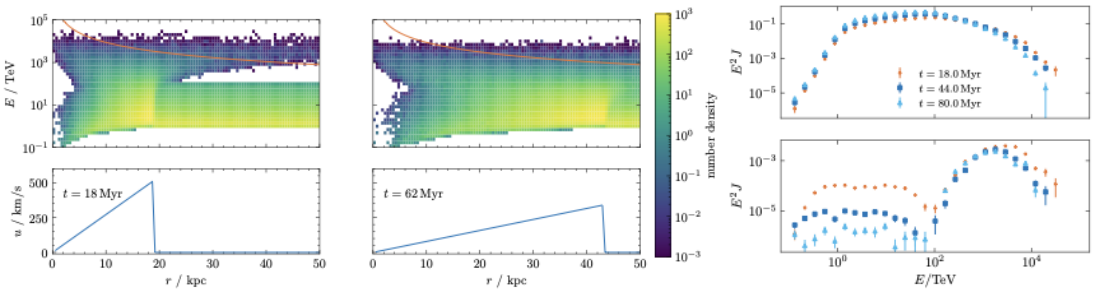

Figure 3: Left: Particle distribution in space and energy (top) and shock profile (bottom) at two times: $t = 18\,\mathrm{Myr}, 62\,\mathrm{Myr}$. Right: Energy spectra $J = \mathrm{d}N/\mathrm{d}E$ at the shock (top) and at the Galactic boundary (bottom) over time and weighted with E^2. Figures taken from [3].

interactions are not considered thus that the result can be applied to heavier particles with the same rigidity as well. Figure 3 shows the velocity profile $u(r,t)$ and the distribution in energy and space at two times $t = 18\,\mathrm{Myr}$, $t = 62\,\mathrm{Myr}$ in the left panel. Note that the region $E = [\mathrm{TeV}, 100\,\mathrm{TeV}]$ for $r > R_{\mathrm{sh}}$ is the injected spectrum. The orange line indicates the maximal energy at which particles are still expected to be diffusive at the scales of the shock. The spectra at the shock and at the Galactic boundary are shown in the right panel of fig. 3.

The spectrum at the shock is almost stationary and can be divided in three parts: The injected energy range $E_{\mathrm{inj}} = [\mathrm{TeV}, 100\,\mathrm{TeV}]$, the cooled energy range $E_{\mathrm{cool}} < \mathrm{TeV}$, and the re-accelerated range $E_{\mathrm{acc}} > 100\,\mathrm{TeV}$. The injected energy range becomes harder over time due to the finite injection range: low energy particles are accelerated up to higher energies and increase the flux. Due to the finite injection range, the loss of accelerated particles at such energies cannot be compensated by the particles accelerated up from even lower energies. As expected, the re-accelerated energy range has a spectral slope < -2, which becomes softer with increasing energy, before the cut-off due to finite acceleration time. The spectrum that escapes back to the Galaxy can be divided into the injected part that is cooled and advected outwards over time, and the high-energy re-accelerated part that is able to diffuse back. While the low energy part decays over time, the re-accelerated part is less affected by advection and is almost stationary.

3.2 Colliding shocks

We further consider two one-dimensional planar shocks that are propagating after each other; the second shock could be launched in the proximity some time after the first. In a 1D planar geometry, second shock must be considerably faster than the first to fulfill the Rankine-Hugoniot conditions, thus that they will always catch up with each other. What happens when they collide? A new Riemann problem emerges, with the undisturbed medium on one side and the twice shocked medium on the other. In between forms a contact discontinuity and a rarefaction wave travels backwards. For this scenario, an analytical wind profile can be constructed analogously to the Sod's shock tube problem, often used as a test case for hydrodynamic codes. The system becomes interesting when the two shocks approach each other, since particles with a large mean-free path could encounter both shocks, which increases the effective compression ratio, giving rise to harder spectrum. However, there is a limited range depending on the diffusive length scale - allowing particles to see both shocks in a given time before they collide - and the acceleration time scale -

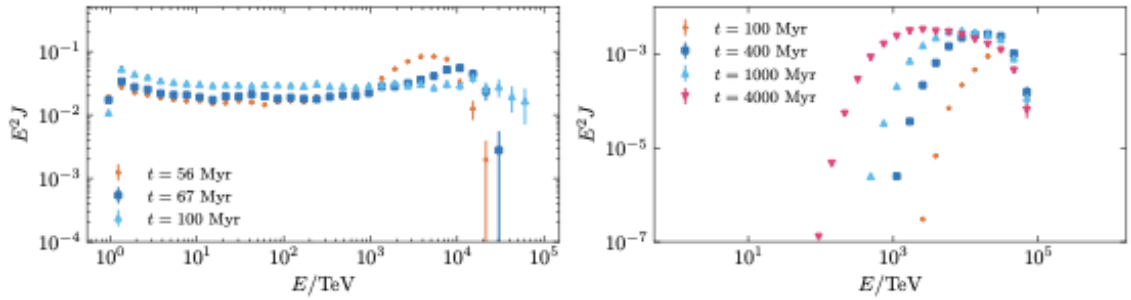

Figure 4: Left: Weighted energy spectra at the single shock after the collision at $t = 50$ Myr. Right: Spectra at the Galactic boundary at differences times after the outflow stopped. Figures taken from [3].

allowing particles to be accelerated in that time. We find that in a short period before the shocks collide the spectrum at high energies becomes harder. This, however, is a transient effect as particles are soon accelerated by the single shock after merger only which produces a -2 spectrum. The spectra at the single shock *after the collision* are shown in fig. 4 at different times.

3.3 Time-dependent escape

Considering the planar shocks from the previous section, without additional cooling particles would not have a chance to propagate back to the Galaxy, even though they escape the shock *downstream*, the downstream frame now moves with the shock speed out of the Galaxy. However, such a strong outflow is not expected to be sustained forever and at some point it will cease. In that case, the time-dependent spectra can simply be calculated by employing the Greens function of the diffusion equation (neglecting potential loss processes). The spectra that would arrive at the Galactic boundary ($z = 5$ kpc) over time are shown in fig. 4 considering a Bohm diffusion coefficient. We note that the energy range of the spectrum that makes it back in a given time strongly depends on the diffusion coefficient (as expected) and that the energy-dependent diffusion gives rise to hard spectra: High-energy particles reach the Galactic boundary first, only after some time the low energy particles follow. This effect reverses at some point, as the mean-square displacement of the high-energy particles is larger than for the low-energy particles, it is more likely to find the latter at the Galactic boundary. The result is a softer spectrum as visible in the last times (pink triangles) shown in fig. 4.

4. Superdiffusive shock acceleration

In case of superdiffusion the escape probability at the shock changes: due to the heavy power-laws of the jump length distribution, particles can make it back to the shock from far downstream. As a result, at the same time more particles are upstream of the shock compared to normal diffusion where the jump length distribution is represented by a Gaussian function. Figure 5 shows the spatial distribution in the shock region, considering a fractional dimension $\alpha = 1.7$ and a (normalized) fractional diffusion coefficient $\kappa_\alpha = 1$.

The change in the escape probability results to a change in the slope of the energy spectrum: Since particles are more efficiently transported back over the shock, the spectrum becomes harder

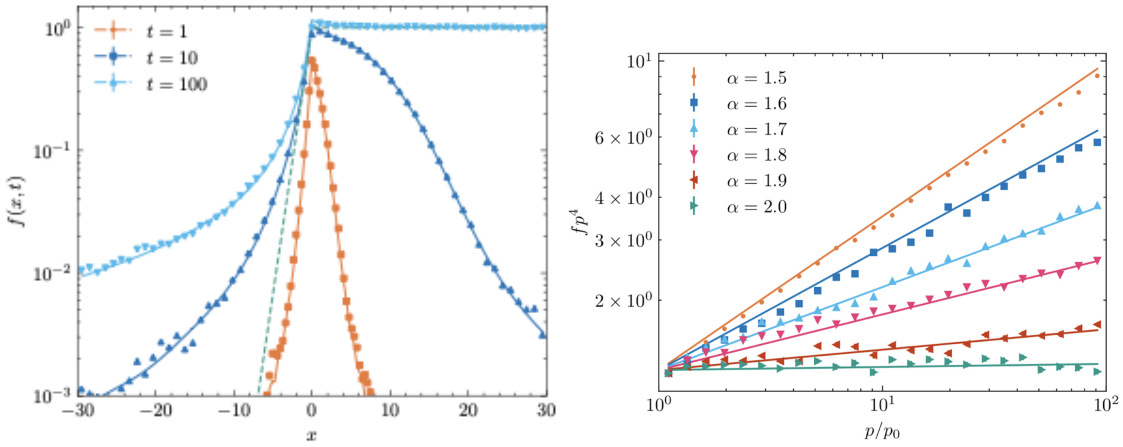

Figure 5: Left: Spatial distribution of particles at the shock in case of superdiffusion with $\alpha = 1.7$, stationary solution in case of normal diffusion is shown by the dashed green line. Right: Resulting spectra at the shock for different frational dimensions, the fitted spectral slope reaches from $s = -2.012 + -0.004$ in case of normal diffusion to $s = -1.576 \pm 0.012$ for $\alpha = 1.5$. Figures taken from [2].

[2]. We find, that considering a constant fractional diffusion coefficient, the slope can become as hard as $s = -1.6$ for a fractional dimension of $\alpha = 1.5$.

5. Summary and Outlook

We presented different advanced models of DSA, all leading to a deviation from the *universal* power-law of -2 at a strong, planar, stationary shock. We considered spherical blast waves, time-dependent escape, colliding shocks and the case of superdiffusion in the shock region.

Acknowledgements

SA, LM, and JT acknowledge support from the Deutsche Forschungsgemeinschaft (DFG): this work was performed in the context of the DFG-funded Collaborative Research Center SFB1491 "Cosmic Interacting Matters - From Source to Signal", project no. 445052434.

References

[1] S. Aerdker et al. *JCAP* **01** (2024) 068
[2] S. Aerdker et al. A&A **693** id.A15, 8 pp. (2025)
[3] S. Aerdker et al. arXiv:2501.14331
[4] R. Alves Batista et al. JCAP **09** 035 (2022)
[5] D. Caprioli JCAP, **07**, 038 (2012)
[6] R. Diesing and D. Caprioli The APJ, **922**, Issue 1, id.1, 11 pp. (2021)
[7] E. A. Dorfi and D. Breitschwerdt A&A **540** id.A77, 15 pp. (2012)
[8] L. O. Drury Reports on Progress in Physics, Volume 46, Issue 8, pp. 973-1027 (1983)
[9] Effenberger et al. A&A **686** id.A219, 7 pp. (2024)
[10] B. Eichmann and M. Kachelrieß, JCAP, **02**, 053 (2023)
[11] E. Fermi Phys. Rev., **75**, Issue 8, pp. 1169-1174 (1949)
[12] L. Merten and S. Aerdker CPC **311** id.109542
[13] L. Merten et al. JCAP **06** 046 (2017)
[14] F. Rieger and P. Duffy ApJL, **886**, Issue 2, article id. L26, 4 pp. (2019)